Simultaneous In Vitro Assay of the First Four Enzymes in the Fungal Aspartate Pathway Identifies a New Class of Aspartate Kinase Inhibitor

David C. Bareich, Ishac Nazi,
and Gerard D. Wright*
Antimicrobial Research Centre
Department of Biochemistry
McMaster University
1200 Main Street
West Hamilton, Ontario L8N 3Z5
Canada

Summary

The biosynthesis of amino acids derived from Asp (Met, Thr, and Ile) is a target for antifungal agents. We have developed a simultaneous in vitro assay of the first four enzymes of the fungal aspartate pathway: aspartate kinase, aspartate semialdehyde dehydrogenase, homoserine dehydrogenase, and homoserine O-acetyltransferase. This reconstructed pathway assay was initiated with the readily accessible amino acid L-Asp and thus circumvents the obstacles of substrate availability and stability for aspartate semialdehyde dehydrogenase and homoserine dehydrogenase. The assay was shown to be suitable for high-throughput screening of chemical libraries for the identification of inhibitors of all four component enzymes. A screen of a library of 1000 small molecules identified a novel class of 7-chloro-4([1,3,4]thiadiazol-2-ylsulfanyl)-quinoline aspartate kinase inhibitors that have the potential to act as leads in the development of new antifungal agents.

Introduction

The fungal aspartate pathway is required for the biosynthesis of threonine, isoleucine, and methionine (Figure 1). The first step in this process is activation of aspartate by phosphorylation catalyzed by aspartate kinase (AK). Using NADPH, aspartate semialdehyde dehydrogenase (ASD) then reduces aspartyl-4-phosphate to aspartate-4-semialdehyde. In the next step, homoserine dehydrogenase (HSD) catalyzes the reduction of aspartate semialdehyde to generate the alcohol homoserine by using either NADPH or NADH. Homoserine sits at a junction in the pathway: phosphorylation by homoserine kinase commits the carbon skeleton to biosynthesis of threonine and isoleucine, whereas acetylation by homoserine O-acetyltransferase (HSAT) commits it to methionine biosynthesis.

The pathway is a good target for new antifungal agents because it is required for fungal viability and is not found in mammals, which is why threonine, isoleucine, and methionine must be obtained from the mammalian diet. Additionally, the essentiality of the pathway has been chemically validated as the natural products azoxybacillin [1], rhizocticin [2], and 2-amino-5-hydroxy-4-oxopen-

*Correspondence: wrightge@mcmaster.ca

tanoic acid [3] have been shown to target homocysteine synthase [4], threonine synthase [5], and HSD [6], respectively, and inhibit the growth of fungi (Figure 1). The importance of this pathway in fungi and other microbes has resulted in a number of studies to identify and characterize inhibitors of various component enzymes [7–10].

With this in mind, we sought to identify other compounds from a chemical library that could inhibit the fungal aspartate pathway. This could be achieved by separately screening the library against each enzyme in the pathway. However, this is costly in terms of the chemicals themselves, time, substrates, and other materials. Furthermore, (1) it is not readily possible to screen ASD in the metabolically relevant direction as its substrate, aspartyl-4-phosphate, is unstable, and (2) HSD uses aspartate-4-semialdehyde, which is not commercially available and must be chemically synthesized. To obviate these problems, we designed a pathway assay whereby the first four enzymes, leading to methionine biosynthesis, are assayed simultaneously (Figure 2). Such an in vitro pathway assay has the obvious advantages of time and cost savings, but also, each additional enzyme screened simultaneously increases the likelihood that an inhibitor may be found from a given set of compounds in a single screen [11]. A pathway assay may also maintain protein-protein interactions that occur in vivo, which may be important for the function of the enzymes. Such interactions have been found in the *Escherichia coli* aspartate pathway enzymes aspartate semialdehyde dehydrogenase and the bifunctional aspartate kinase I–homoserine dehydrogenase I, which facilitate substrate shuttling of the unstable intermediate aspartyl-4-phosphate [12]. Finally, the pathway assay also allows the identification of compounds, which in principle could be metabolized by the enzymes in the pathway to new forms that have inhibitory activity [13].

Results and Discussion

The first four enzymes of the fungal aspartate pathway were empirically linked together to establish the assay in progressive steps, starting with *Saccharomyces cerevisiae* AK (AK_{Sc}). AK_{Sc} was assayed for adenosine diphosphate (ADP) production by coupling to pyruvate kinase and lactate dehydrogenase (PK-LDH). Sequential additions of the *S. cerevisiae* enzymes ASD (ASD_{Sc}) and HSD (HSD_{Sc}), which were both assayed by monitoring NADPH oxidation, and *Schizosaccharomyces pombe* HSAT ($HSAT_{Sp}$), assayed for CoASH production, were optimized such that AK_{Sc} was rate limiting, and the additional enzymes were present at levels that would sustain rates just exceeding that set by AK_{Sc}. To ensure that these criteria were being met at each optimized step, the steady-state kinetic parameters and the L-Thr IC_{50} of AK_{Sc} were assessed prior to optimizing a subsequent step (Table 1). With the exception of the ATP K_m values, which varied 5-fold, the remaining parameters for AK_{Sc} were similar after optimizing each step, indicating that
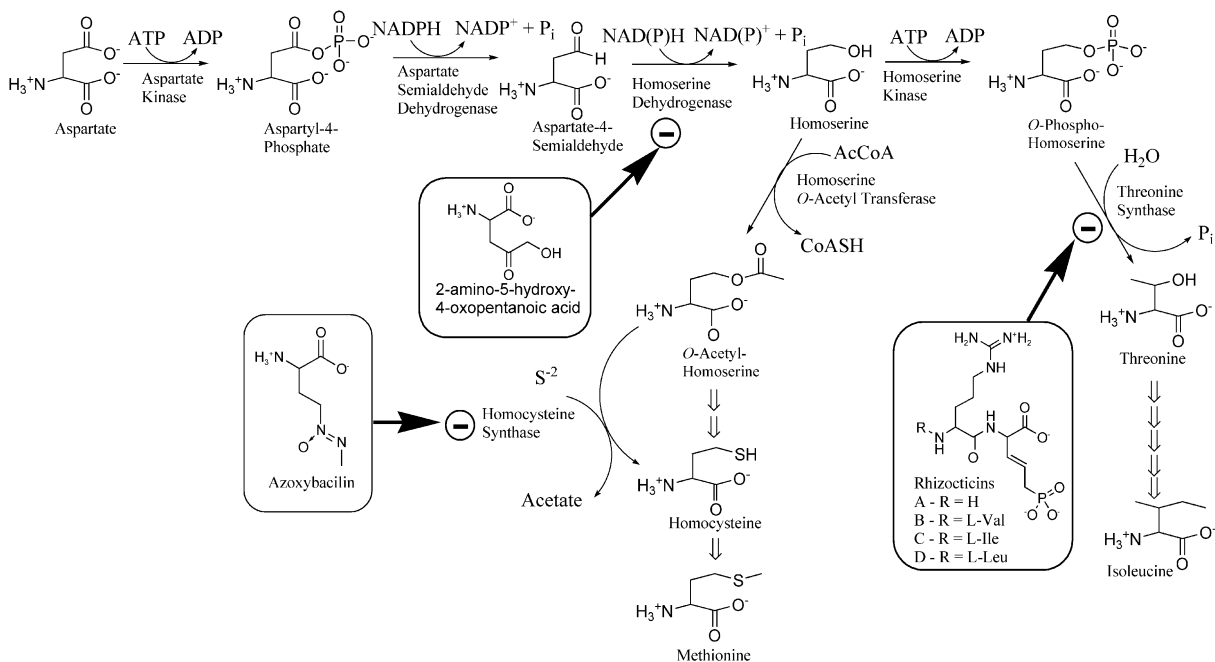
Figure 1. The Fungal Aspartate Pathway Showing the Sites of Action of the Natural Product Inhibitors Azoxybacillin, the Rhizocticins, and 2-amino-5-hydroxy-4-oxopentanoic Acid

AK_{Sc} remained rate limiting. To establish the ability of the pathway assay to respond to inhibitors of AK_{Sc}, HSD_{Sc}, and $HSAT_{Sp}$, IC_{50}s of known inhibitors of each enzyme were determined using the pathway assay (Table 1). These include the AK inhibitors L-Thr and β-hydroxynorvaline [14], the HSD inhibitor 3-*tert*-butyl-4-hydroxyphenyl sulfide (L. Ejim and G.W., unpublished data), and the HSAT inhibitor 2,3-dibromomalonamide (I.N. and G.W., unpublished data). In all cases, IC_{50}s were found to be within 2-fold of the values determined in assays of the individual enzymes, establishing the ability

of the pathway assay to identify compounds that inhibit any of the enzymes present.

High-throughput screens must be robust to maximize the chances of identifying inhibitory compounds and minimize false positives. One way to visualize the robustness of the assay is to analyze a significant number of positive (100% activity) and negative (0% activity) controls obtained during the screen. The spread of the data values between an arbitrary cutoff of three standard deviations between both positive and negative controls provides a measure of quality of the assay and its use-
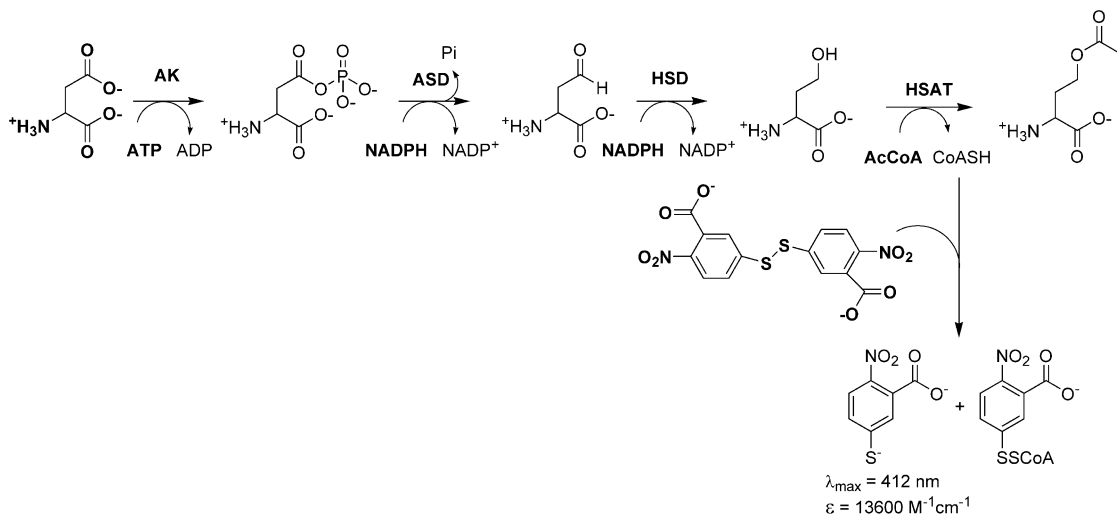

Figure 2. The Assay of the First Four Enzymes in the Fungal Aspartate Pathway

Reagents added to the assay mixture are indicated in bold.

Table 1. Optimization and Inhibition of Enzyme Throughput

Linked Enzymes	ATP		Asp		Inhibitor	IC$_{50}$(mM)	Target Enzyme
	K_m(mM)	k_{cat}(s^{-1})	K_m(mM)	k_{cat}(s^{-1})			
AK$_{Sc}$-PK-LDH	1.3	40	3.3	36	L-Thr	3.4	AK
AK$_{Sc}$-ASD$_{Sc}$	0.5	49	2.5	36	L-Thr	4.5	AK
AK$_{Sc}$-ASD$_{Sc}$-HSD$_{Sc}$	2.3	50	3.4	43	L-Thr	3.6	AK
AK$_{Sc}$-ASD$_{Sc}$-HSD$_{Sc}$-HSAT$_{Sp}$	0.5	45	3.4	50	L-Thr	4.0	AK
AK$_{Sc}$-ASD$_{Sc}$-HSD$_{Sc}$-HSAT$_{Sp}$					(structure)	5.3	AK
AK$_{Sc}$-ASD$_{Sc}$-HSD$_{Sc}$-HSAT$_{Sp}$					(structure)	0.0073	HSD
AK$_{Sc}$-ASD$_{Sc}$-HSD$_{Sc}$-HSAT$_{Sp}$					(structure)	0.0048	HSAT

Inhibitor controls and AK$_{Sc}$ steady-state kinetic parameters for each step in the development of the pathway assay.

fulness in screening, which we term the screening window (Figure 3A). The statistical parameter Z′ reports quantitatively on the data variation and provides a means of assessing the quality of the screen. The Z′ factor (see Equation 3 in Experimental Procedures) was determined to be 0.65, indicating that the screening window can reliably identify enzyme inhibitors [15].

The results of a screen of the pathway assay in duplicate against a 1000-compound chemical library at a concentration of 10 μM are shown graphically (Figure
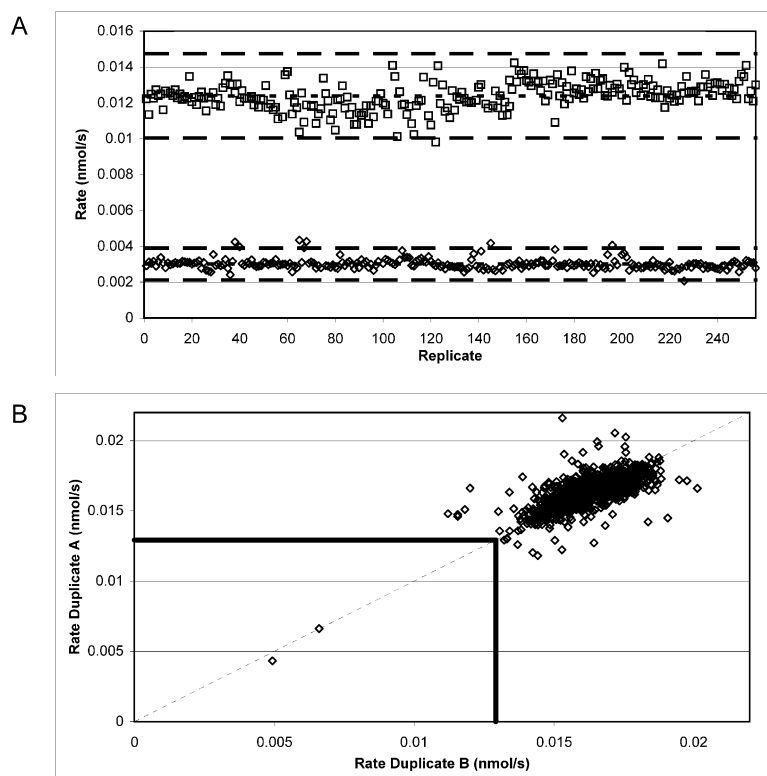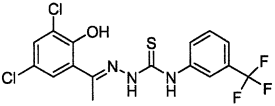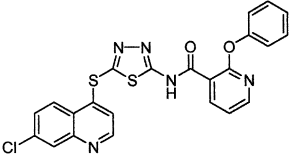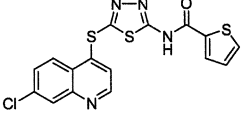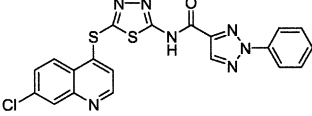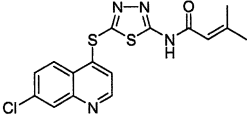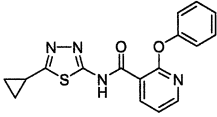

Figure 3. Evaluation of In Vitro Asp Pathway Screen

(A) Plot of 100% (□) and 0% (◇) activity controls for the high-throughput screen. Dashed lines indicate the average for the controls; heavy dashed lines indicate three standard deviations. The screening window is located between the inner three standard deviation lines for the 100% and 0% activity controls, at approximately 0.01 and 0.004 nmol/s, respectively.

(B) Results of the screen of a library of 1000 small molecules against the pathway assay. Duplicate values for each compound are plotted on opposing axes, if the duplicates are in agreement they should fall on a line with a slope of 1 (dashed line). Three standard deviations below the average result is considered to be statistically significant inhibition and is demarked by thick lines.

Table 2. SAR of 7-chloro-4([1,3,4]thiadiazol-2-ylsulfanyl)-quinoline Aspartate Kinase Inhibitors Identified in the Screen

	Compound	IC_{50} (μM)
	1	18 $\pm$ 3.7
	2	3.1 $\pm$ 0.8
	3	3.6 $\pm$ 0.8
	4	1.6 $\pm$ 0.7
	5	n.i.[a]
	6	n.i.[a]

[a] No inhibition observed at a concentration of 30 μM.

Table 3. Identification of the Enzyme Inhibited by Compound 2

Linked Enzymes	IC_{50} (μM)
AK_{Sc}-ASD_{Sc}-HSD_{Sc}-$HSAT_{Sp}$	3.1 $\pm$ 0.52
AK_{Sc}-ASD_{Sc}-HSD_{Sc}	12 $\pm$ 4.3
AK_{Sc}-ASD_{Sc}	12 $\pm$ 2.5
AK_{Sc}-PK-LDH	3.1 $\pm$ 0.78

3B). To assess the reproducibility of the duplicate assay, a plot of the activity remaining in the presence of each compound for each duplicate assay was constructed where the x and y coordinates for each data point are the first and second values, respectively, determined for each compound (Figure 3B). If the duplicates are in perfect agreement they will fall on a line with a slope of one and a bias in the assay would be indicated by a nonrandom distribution of the results about this line. Three standard deviations below the average value was used as the statistically significant cutoff to define a compound as being an inhibitor of the assay. Using these criteria, the screen identified two compounds as reproducible inhibitors from the 1000-compound chemical library.

The structures of the compounds identified in the screen, a thiourea substituted with 2,4-dichlroro-6-(1-imino-ethyl)-phenol and 3-trifluromethylphenyl groups (1) and N-[5-(7-chloro-quinolin-4-ylsulfanyl)-[1,3,4]thiadiazol-2-yl]-2-phenoxy-nicotinamide (2), are shown in Table 2. To empirically determine which pathway enzyme was inhibited by compounds 1 and 2, IC_{50}s were determined for all sequential combinations of the path-

way beginning with AK_{Sc}, as well as the assay for ADP production by AK_{Sc} (Table 3). Because IC_{50} values were obtained from all sequential combinations of the pathway and the values were within 4-fold of each other, both compounds were concluded to be AK_{Sc} inhibitors.

We investigated the mode of AK_{Sc} inhibition and K_i values for 1 and 2 by using an AK_{Sc}-ASD_{Sc} coupled assay to look for NADPH oxidation. Double reciprocal plots for the inhibition of AK_{Sc} by 1 versus both substrates appeared to be competitive; however, attempts to fit the data to any standard model of inhibition were unconvincing (data not shown). Furthermore, close structural analogs of 1 showed no inhibition of AK at concentrations of 30 μM, therefore, given this weak activity, we elected not to pursue further evaluation of this compound.

On the other hand, compound 2 was found to be a reversible inhibitor of AK_{Sc}. Analysis of the steady-state inhibition data revealed that 2 fit best to a model of partial noncompetitive inhibition of ATP (K_i, 3.6 $\pm$ 0.22 μM; β, 0.31 $\pm$ 0.01) and partial mixed inhibition of L-Asp (K_i, 4.0 $\pm$ 0.85 μM; α, 0.50 $\pm$ 0.11; β, 0.33 $\pm$ 0.02) (Figure 4). These models of inhibition suggest that 2 may be binding at a site that does not overlap with either substrate and where the enzyme•substrate•inhibitor complex can still produce product but at an impaired rate [16]. Compounds 1 and 2 had no effect on the growth of S. cerevisiae DL1, Candida parapsilosis ATCC 90018, and Candida albicans ATCC 90028 in minimal RPMI liquid media at concentrations up to 64 μg/mL. This could be the result of the μM affinity of the compounds or reflect membrane transport or efflux problems.

Structural analogs of 2 were identified in an in silico substructure search of a 50,000-compound chemical library from Maybridge plc. IC_{50}s were determined using the AK_{Sc}-PK-LDH assay for each analog to determine what structural features were important for inhibition of AK_{Sc} (Table 2). Two analogs of 2 that maintain the core 7-chloro-4([1,3,4]thiadiazol-2-ylsulfanyl)-quinoline structure, 3 and 4, showed IC_{50}s similar to the parent compound, indicating that the 2-phenoxypyridine group can be replaced by other heterocycles. This portion of the molecule is important for enzyme affinity as 5, in which the 2-phenoxypyridine is replaced by an isobutene group, shows no interaction with the enzyme at 30 μM, the highest concentration tested (Table 2). Similarly, the 4-thio-7-chloroquinoline group was also essential, as the replacement with a cyclopropane group (compound 6) results in loss of activity (Table 2).

Significance

We have designed and optimized a pathway assay of the first four enzymes in the fungal aspartate pathway
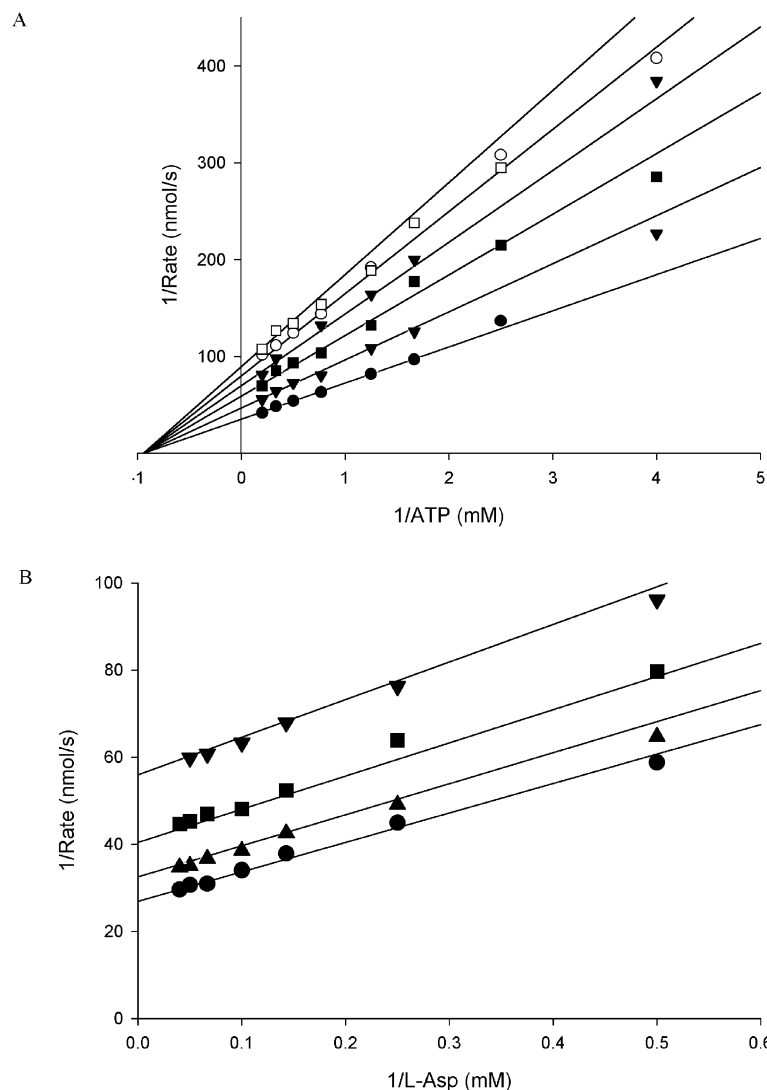
A

B

Figure 4. Inhibition of AK_{Sc} by Compound 1

Double reciprocal plots for the inhibition of AK_{Sc} by 1.
(A) 1 versus ATP. Concentration of 1: ●, 0 μM; ▼, 2 μM; ■, 5 μM; ▼, 9 μM; ○, 15 μM; □, 25 μM.
(B) 1 versus L-Asp. ●, 0 μM; ▲, 0.7 μM; ■, 2 μM; ▼, 7 μM. The activity of AK_{Sc} was monitored by coupling aspartyl-4-phosphate production to ASD_{Sc}, as described in Experimental Procedures.

for use in high-throughput screening of chemical libraries. The aspartate pathway is a good target for new antifungal agents, as it is not found in mammals and is required for fungal viability shown by several natural products, which inhibit the pathway. This work has demonstrated that this pathway assay is amenable to high-throughput screening, which has several advantages over separately screening each enzyme, including time and cost improvements, but also the ability to screen ASD_{Sc} and HSD_{Sc} in the metabolically relevant direction. This pathway assay enabled the identification of a new class of inhibitors of fungal AK, and structure activity analysis revealed structural constraints for inhibition. These are the first reported non-amino acid inhibitors of fungal AK and as such could serve as leads in new antifungal compound development.

Experimental Procedures

**Cloning, Expression, and Purification of Fungal
Aspartate Pathway Enzymes**
Cloning, expression, and purification of AK_{Sc} and HSD_{Sc} are described elsewhere [17].

The *HOM2* gene encoding ASD_{Sc} was amplified from *S. cerevisiae* genomic DNA via the polymerase chain reaction with the oligonucleotide primers 5′-GGTGGTCATATGGCTGGAAAGAAAATTGCTGG and 5′-CCGCTCGAGGGATCCTTAAATCAAGTTTCTTGCTAGTAAGATT TCGG. We cloned the amplified fragment into the NdeI and XhoI restriction sites by using standard techniques. The resulting DNA sequence-confirmed plasmid, pET28 + ASD_{Sc}, was transformed into *E. coli* BL21(DE3) cells allowing expression of ASD_{Sc} with an N-terminal hexa-histidine tag.

The His-tagged enzyme was expressed in *E. coli* BL21(DE3)/ pET28 + ASD_{Sc} by growing two 1 liter cultures in LB, supplemented with 50 μg/mL kanamycin to an OD_{600} of 0.6 at 37°C. The cultures were cooled in an ice water bath to 16°C, isopropyl β-D-1-thiogalactopyranoside (IPTG) was added to a final concentration of 1 mM, and incubated overnight at 16°C in an orbital shaker at 250 rpm. Cells were harvested by centrifugation at 13,000 × *g* for 10 min, the cell pellet was resuspended in 20 ml of 20 mM 4-(2-hydroxyethyl)piperazine-1-ethanesulfonic acid (HEPES) (pH 8.0), and lysed with three passes through a French pressure cell at 10,000 psi in the presence of 1 mM phenylmethylsulfonyl fluoride. Following centrifugation for 10 min at 43,000 × *g*, the supernatant was applied on to a 5 ml Ni NTA Agarose column, the column was washed with 20 mM HEPES (pH 8.0) until the OD_{280} decreased to less than 100 mAu, and the bound protein was eluted with a gradient of 0–100 mM imidazole in 20 mM HEPES (pH 8.0). Active fractions were identified immediately, pooled, and dialyzed overnight against 4 liters of 20

mM HEPES (pH 8.0). The dialyzed enzyme was concentrated and frozen at $-80°C$ with 10% glycerol.

We had difficulties producing HSAT from *S. cerevisiae* in sufficient quantity and quality for these studies and therefore elected to produce the 66% homologous (50% identical) enzyme from *S. pombe*. The *MET2* gene encoding HSAT$_{Sp}$ was amplified from *S. pombe* genomic DNA using the oligonucleotide primers 5′-GGGAATTCCA TATGGAATCTCAATCTCCGATTGAATCAATTGTCTTTAC and 5′-CGC GGATCCAAGCTTTTACCAGGAGGTTATGTCTTCCATTTCTC. The amplified fragment was cloned into the NdeI and HindIII restriction enzyme sites of pET28 by using standard techniques, and the DNA sequence was verified. The resulting plasmid, pET28 + HSAT$_{Sp}$, was transformed into *E. coli* BL21(DE3) cells allowing the expression of HSAT$_{Sp}$ with an N-terminal hexa-histidine tag.

The His-tagged enzyme was expressed in *E. coli* BL21(DE3)/ pET28 + HSAT$_{Sp}$ in 1 liter of LB supplemented with 50 μg/mL kanamycin to an OD$_{600}$ of 0.6 at 37°C. The cultures were cooled in an ice water bath to 16°C, IPTG was added to a final concentration of 1 mM, and were incubated for 2 hr at 16°C in an orbital shaker. The cultures were harvested by centrifugation at 13,000 × *g* for 10 min, and the cells from four 1L cultures resuspended in 30 ml of 20 mM HEPES (pH 8.0), and lysed with three passes through a French pressure cell at 10,000 psi. Cell debris was pelleted at 43,000 × *g* for 10 min and the supernatant was loaded on a 15 ml Ni NTA Agarose column. The column was washed until the OD$_{280}$ decreased to less than 100 mAu, and the bound HSAT$_{Sp}$ was eluted with 10 ml of 100 mM imidazole in 20 mM HEPES (pH 8.0) directly onto a 20 ml Q Sepharose column, which was washed similarly and eluted with a gradient of 0–400 mM NaCl in 20 mM HEPES (pH 8.0). HSAT$_{Sp}$ active fractions were pooled and found to yield 20 mg of pure HSAT$_{Sp}$.

ADP Production Assay

AK$_{Sc}$ activity was determined by coupling production of ADP with the lactate dehydrogenase-dependent oxidation of reduced NADH in the presence of phosphoenol pyruvate and pyruvate kinase. Reaction mixtures contained 7 mM ATP, 0.33 U pyruvate kinase, 0.66 U lactate dehydrogenase, 2.5 mM phosphoenol pyruvate, 1 mM NADH, 10 mM KCl, 40 mM MgSO$_4$, 100 mM HEPES (pH 7.5) in a final volume of 100 μl contained in a 96 well flat bottom microtitre plate. A 6 min preincubation was used to ensure that any contaminating ADP was regenerated to ATP as well as allowing for temperature equilibration to 30°C. The reactions were initiated with the addition of at least 25 mM L-aspartate and monitored at 340 nm in a Molecular Devices Spectramax microtitre platereader. For steady-state kinetics, one substrate was held fixed while the other was varied at eight substrate concentrations in duplicate, ranging from 0.4 to 7 mM for ATP and 0.5 to 30 mM L-Asp. Data were fit to Equation 1 for Michaelis-Menten kinetics using the computer program GraFit [18].

$$\upsilon = \frac{V_{max}S}{(K_m + S)} \qquad (1)$$

L-Threonine IC$_{50}$ Determinations

Assays were similar to assays for ADP production, with the addition of L-threonine concentrations ranging from 0.05 to 150 mM; ATP and L-Asp were present at 5 and 12.5 mM, respectively. Data were fit to the four-parameter Equation 2, using GraFit [18] to solve for the IC$_{50}$, where A = minimum response plateau, D = maximum response plateau, I = concentration of inhibitor, and S = slope factor.

$$y = \frac{A - D}{1 + \left(\dfrac{I}{IC_{50}}\right)^S} + D \qquad (2)$$

NADPH Oxidation Assay

NADPH oxidation by ASD$_{Sc}$ separately or with HSD$_{Sc}$ was monitored at 340 nm ($\epsilon_{340\,nm}$ = 6300 M^{-1}cm^{-1}). Conditions for this assay are identical to those for ADP production with the substitution of ASD$_{Sc}$ alone or in combination with HSD$_{Sc}$ for PK-LDH.

Assay for CoASH Production

HSAT$_{Sp}$ production of CoASH was by monitored by in situ titration of 5,5′-dithiobis-(2-nitrobenzoic acid) (DTNB) [19]. Production of the mixed disulfide of CoASH-5-thio-2-nitrobenzoic acid and release of the chromophoric thiolate was monitored at 412 nm ($\epsilon_{412\,nm}$ = 13600 M^{-1}cm^{-1}) (Figure 2). The assay was buffered with 100 mM HEPES (pH 7.0) and contained 40 mM MgSO$_4$, 10 mM KCl, 0.8 mM ATP, 1.2 mM NADPH, and 0.2 mM AcCoA and the optimized amounts of AK$_{Sc}$, ASD$_{Sc}$, HSD$_{Sc}$, and HSAT$_{Sp}$. The pathway assay reactions were initiated by the addition of a mixture of L-Asp and DTNB, such that final concentrations were 6 and 0.22 mM, respectively. Zero percent activity controls were identical in every respect except for the absence of L-Asp. Assays were monitored at 412 nm for a minimum of 5 min at 30°C. Similar assays were used for the purification of HSAT$_{Sp}$ except reactions were initiated with L-homoserine and DTNB, avoiding the need for the other pathway enzymes and their substrates.

Optimization of the Pathway Assay

The amount of AK$_{Sc}$ yielding an easily measured progress curve (slope approximately 20–30 times above background) that was linear for at least 5 min was determined by titrating AK$_{Sc}$ and assaying for ADP production. The amount of ASD$_{Sc}$ sufficient to just exceed the rate established by AK$_{Sc}$ was determined empirically by varying ASD$_{Sc}$ while keeping AK$_{Sc}$ constant and assaying for NADPH oxidation. The amount of HSD$_{Sc}$ was optimized in a similar manner as for ASD$_{Sc}$; however, the observed slope was twice that found for ASD$_{Sc}$, because the stoichiometry of NADPH consumption had doubled due to the added dehydrogenase activity of HSD$_{Sc}$. To reduce expense, the concentration of NADPH was kept to a minimum, 1.2 mM, without becoming rate limiting. The amount of HSAT$_{Sp}$ was optimized in a similar manner using the assay for CoASH production. Observed activity was found to decrease with increasing concentrations of DTNB, likely due to inactivation of one of the pathway enzymes by DTNB, therefore this reporter molecule was added at a concentration just exceeding the limiting substrate concentration with the initiating substrate L-Asp. After each additional enzyme was optimally linked, the AK$_{Sc}$ steady-state kinetic parameters along with the L-Thr IC$_{50}$ were determined to confirm that the rate-limiting step remained AK$_{Sc}$.

Enzyme Screening

Compounds from the Maybridge collection were dissolved at 200 μM in dimethyl sulfoxide in 96 well microtitre plates. Compounds, sufficient for a 10 μM final concentration, and master mix containing buffer, Mg^{2+}, enzymes, and substrates were transferred to the assay plate and preincubated 15 min at 30°C in concentrations identical to the assay conditions for CoASH production. Reactions were initiated by the addition of a mixture of L-Asp and DTNB, such that final concentrations were 6 and 0.22 mM, respectively. Assays were monitored at 412 nm for 5 min at 30°C.

The identity of compounds 1 and 2 derived from the screen was verified by liquid chromatography with mass spectrometry detection.

Data Analysis and Characterization of Inhibitory Compounds

The quantitative measure of the quality of the assay, called the Z′ factor, was calculated for the assay (Equation 3 [15]).

$$Z'\ factor = 1 - \left[\frac{3\sigma_{high} + 3\sigma_{low}}{(average_{high} - average_{low})}\right] \qquad (3)$$

Equation 2 was used for determining IC$_{50}$ values for the various inhibitory compounds.

The mode of inhibition of AK$_{Sc}$, K_i value, and reversibility of inhibition by hits derived from the primary screen was determined. To assess the mode of inhibition, double reciprocal plots were generated with individual lines fit to a simple double reciprocal model, Equation 4, and the type of inhibition confirmed by F test comparing global fits of the data to various models of inhibition, including hyperbolic noncompetitive (Equation 5) and hyperbolic mixed inhibition, (Equation 6). Inhibition constants were obtained from the global fit to the appropriate model, using the enzyme kinetics module of Sigma Plot [20]. Reversibility of inhibition was determined by com-

paring activity of AK_{Sc} plus an inhibitor concentration providing 50% inhibition to an AK_{Sc} control at 50% of the uninhibited activity following 6 min incubation at 30°C, diluting to various volumes, and starting the reaction with the same concentrations of all other components in the ADP production assay.

$$\frac{1}{v} = \frac{1}{V_{max}} + \frac{K_m}{V_{max}S} \tag{4}$$

$$v = \frac{V_{max}}{\left(\left(1 + \frac{K_m}{S}\right) \times \frac{\left(1 + \frac{I}{K_i}\right)}{\left(1 + \frac{\beta I}{K_i}\right)}\right)} \tag{5}$$

$$v = V_{max} \times \frac{\frac{\left(1 + \frac{\beta I}{(\alpha K_i)}\right)}{\left(1 + \frac{I}{(\alpha K_i)}\right)}}{\left(1 + \frac{K_m}{S}\right) \times \frac{\left(1 + \frac{I}{K_i}\right)}{\left(1 + \frac{I}{(\alpha K_i)}\right)}} \tag{6}$$

Acknowledgments

References

1. Fujiu, M., Sawairi, S., Shimada, H., Takaya, H., Aoki, Y., Okuda, T., and Yokose, K. (1994). Azoxybacilin, a novel antifungal agent produced by *Bacillus cereus* NR2991. Production, isolation and structure elucidation. J. Antibiot. (Tokyo) *47*, 833–835.

2. Kugler, M., Loeffler, W., Rapp, C., Kern, A., and Jung, G. (1990). Rhizocticin A, an antifungal phosphono-oligopeptide of *Bacillus subtilis* ATCC 6633: biological properties. Arch. Microbiol. *153*, 276–281.

3. Yamaguchi, H., Uchida, K., Hiratani, T., Nagate, T., Watanabe, N., and Omura, S. (1988). RI-331, a new antifungal antibiotic. Ann. N Y Acad. Sci. *544*, 188–190.

4. Aoki, Y., Kondoh, M., Nakamura, M., Fujii, T., Yamazaki, T., Shimada, H., and Arisawa, M. (1994). A new methionine antagonist that has antifungal activity: mode of action. J. Antibiot. (Tokyo) *47*, 909–916.

5. Laber, B., Gerbling, K.P., Harde, C., Neff, K.H., Nordhoff, E., and Pohlenz, H.D. (1994). Mechanisms of interaction of *Escherichia coli* threonine synthase with substrates and inhibitors. Biochemistry *33*, 3413–3423.

6. Yamaki, H., Yamaguchi, M., Tsuruo, T., and Yamaguchi, H. (1992). Mechanism of action of an antifungal antibiotic, RI-331, (S) 2-amino-4-oxo-5-hydroxypentanoic acid; kinetics of inactivation of homoserine dehydrogenase from *Saccharomyces cerevisiae*. J. Antibiot. (Tokyo) *45*, 750–755.

7. Cox, R.J., Hadfield, A.T., and Mayo-Martin, M.B. (2001). Difluoromethylene analogues of aspartyl phosphate: the first synthetic inhibitors of aspartate semi-aldehyde dehydrogenase. Chem. Commun. (Camb.) *18*, 1710–1711.

8. Cox, R.J., Gibson, J.S., and Mayo Martin, M.B. (2002). Aspartyl phosphonates and phosphoramidates: the first synthetic inhibitors of bacterial aspartate-semialdehyde dehydrogenase. Chembiochem. *3*, 874–886.

9. Kish, M.M., and Viola, R.E. (1999). Oxyanion specificity of Aspartate-beta-semialdehyde Dehydrogenase. Inorg. Chem. *38*, 818–820.

10. Jacques, S.L., Ejim, L.J., and Wright, G.D. (2001). Homoserine dehydrogenase from *Saccharomyces cerevisiae*: kinetic mechanism and stereochemistry of hydride transfer. Biochim. Biophys. Acta *1544*, 42–54.

11. Wong, K.K., Kuo, D.W., Chabin, R.M., Fournier, C., Gegnas, L.D., Waddell, S.T., Marsilio, F., Leiting, B., and Pompliano, D.L. (1998). Engineering a cell-free murein biosynthetic pathway: combinatorial enzymology in drug discovery. J. Am. Chem. Soc. *120*, 13527–13528.

12. James, C.L., and Viola, R.E. (2002). Production and characterization of bifunctional enzymes. Substrate channeling in the aspartate pathway. Biochemistry *41*, 3726–3731.

13. Shames, S.L., Ash, D.E., Wedler, F.C., and Villafranca, J.J. (1984). Interaction of aspartate and aspartate-derived antimetabolites with the enzymes of the threonine biosynthetic pathway of *Escherichia coli*. J. Biol. Chem. *259*, 15331–15339.

14. Ramos, C., and Calderon, I.L. (1992). Overproduction of threonine by *Saccharomyces cerevisiae* mutants resistant to hydroxynorvaline. Appl. Environ. Microbiol. *58*, 1677–1682.

15. Zhang, J.H., Chung, T.D., and Oldenburg, K.R. (1999). A simple statistical parameter for use in evaluation and validation of high throughput screening assays. J. Biomol. Screen. *4*, 67–73.

16. Segel, I.H. (1993). Enzyme Kinetics. (New York: John Wiley & Sons, Inc).

17. Jacques, S.L., Nieman, C., Bareich, D., Broadhead, G., Kinach, R., Honek, J.F., and Wright, G.D. (2001). Characterization of yeast homoserine dehydrogenase, an antifungal target: the invariant histidine 309 is important for enzyme integrity. Biochim. Biophys. Acta *1544*, 28–41.

18. Leatherbarrow, R.J. (2001). GraFit, Version 4.0. Staines, UK Erithacus Software Ltd.

19. Ellman, G.L. (1959). Tissue sulfhydryl groups. Arch. Biochem. Biophys. *82*, 70–77.

20. Brannan, T., Althoff, B., Jacobs, L., Norby, J., and Rubenstein, S. (2000). Sigma Plot, Version 6. Chicago, IL. SSPS, Inc.